

Molecular Modeling Directed by an Interfacial Test Apparatus for the Evaluation of Protein and Polymer Ingredient Function in Situ

GEORGE W. COLLINS, AVANI PATEL, ALAN DILLEY, AND DIPAK K. SARKER*

Chemical Biology Research Group, School of Pharmacy and Biomolecular Sciences, The University of Brighton, Moulsecoomb Science Campus, Lewes Road, Brighton BN2 4GJ, United Kingdom

A simplified apparatus is described that measures the damping of a suspended measuring device. The movement of the device (bob) is damped by the properties of the air–water surface adsorbed material. Its value lies in describing the surface chemomechanical properties of ingredients and excipients used in food, nutraceutical, cosmetic (cosmeceutical), and natural drug–food product formulations that traverse the food sciences. Two surfactants, two food and drug-grade polymers, and five naturally occurring food and serum proteins were tested and used to estimate and model interfacial viscoelasticity. Equilibration times of > 15 min were found to give sufficiently stable interfaces for routine assessment. The viscoelasticity of the air–water interface was estimated with reference to model solutions. These model solutions and associated self-assembled interfacial nanostructured adsorbed layers were fabricated using a preliminary screening process with the aid of a specialized foaming apparatus (C_{300} values), surface tension measurements (23–73 mN/m), and referential surface shear and dilation experiments. The viscoelasticity measured as a percentage of surface damping (D) of a pendulum was found to range from 1.0 to 22.4% across the samples tested, and this represented interfacial viscosities in the range of 0–4630 μ Ns/m. The technique can distinguish between interfacial compositions and positions itself as an easily accessible valuable addition to tensiometric and analytical biochemistry-based techniques.

KEYWORDS: Protein surfactant; damping; viscosity; cross-linking; interface

INTRODUCTION

Food and industrial formulations make use of mixtures of proteins as product functionalizers, polymers, and chemical processing aids such as surfactants and food emulsifiers or lipidic excipients (8, 18). Foods and products having primary ingredients consisting of native and chemically modified food proteins, polysaccharides, and lipids are widespread (6) and can include simple natural foods themselves, “synthetic foods”, and pharmaceutical dispersions (3, 9). The interplay of ingredients and its effect on the macroscopic behavior of food and therapeutic products remains an area of significant interest because of quality and economic considerations. Shelf life and compositional variations are of interest to food manufacturers and processors alike (19, 28). Investigation of the inclusion of antioxidants and interfacial effects on lipid autoxidation in food based on oils (12) is deemed important to the modeling and prediction of product shelf life. The role of new “purpose-built biosurfactants”, food nutrient status, textural properties, and breakdown compounds such as Maillard reaction products becomes an important feature of mass-produced goods that are

based on coarse or nanodispersions. These can include cereals (dough, cakes, confectionary, etc.), milk protein-based dispersions and gels, edible oils, products for parenteral nutrition or therapy, and nutraceutical–cosmeceutical oils and lotions (8).

The notion of competitive adsorption of surfactants and proteins has been studied over a period of time and is illustrated to good effect in surface dilation and foam film experiments (21). Additionally, competitive displacement and adsorption between a synthetic polymer and lauryl sulfate (SDS) soap have also been studied for the purposes of evaluation of binding capabilities (18), and serum albumin–lipid interactions have been studied for use in microencapsulation (that might be extended to food volatiles and flavor) applications (8).

When applied to investigations concerning dispersed product stability, this has been related to the formation of a water cushion covering the polymer or protein and the molecular freedom of the chains on the surface of a colloidal particle that can permit protein attachment (e.g., serum complement system proteins) in the case of polymer-coated drug particles, such as liposomes (9, 26). This response has been observed for ethylene oxide and propylene oxide block copolymers such as pluronics, poly(ethylene glycol), and poly(lactide-*co*-glycolide). The interconversion between a flattened “mushroom” and an upright “brush” surface (and various intermediary) forms of surface adsorbed polymer-

* Author to whom correspondence should be addressed [e-mail d.k.sarker@brighton.ac.uk; telephone +44 (0) 1273 642074; fax +44 (0) 1273 642674].

70 like material is thought to both influence both drug product
71 stability and have a bearing on the stability of protein-based
72 food foams and emulsions (21–24) via steric repulsion, obstruction
73 of contact, and interaction with the entrained foam lamella
74 liquid. With particulate dispersions, protein or polymer dehydration
75 and removal of this water “cushion” lead to aggregation
76 of the particles (3) and subsequent flocculation, and with foams
77 and emulsions this can increase the extent of “natural” creaming
78 and coalescence (23–25). The movement of small molecules,
79 such as emulsifiers, within the gelled adsorbed layer, considered
80 as aggregates or a network with micro- and nanoscale defects
81 (10), can relate to the behavior of complex systems and is
82 thought to affect gross textural properties.

83 The interface, in addition to being interesting in its own right,
84 represents an ideal planar (more simplified) model environment
85 for examination of molecular complexing and cross-linking
86 processes and how they influence food quality in addition to
87 chemical instability and incompatibility. The aim of our work
88 has been to produce a simplified surface rheometer to screen
89 interactions that might occur between surface-active biological
90 and synthetic food polymer molecules in an attempt to supplement
91 sometimes inconclusive spectrophotometric and light-scattering
92 methods and complex bulk rheology. Adsorbed protein is often modeled
93 as a continuous gel network, and the exchange of covalent bonds such as
94 disulfide bonds or ester linkages becomes important. Under appropriate
95 conditions this can be modeled by surface rheology so that elements of
96 chemistry, not simply mechanical properties, can be identified
97 (27).
98

99 Over the past decade a number of impressive techniques, in
100 terms of the labor investment and study required for their setup,
101 have been used to examine interfacial mechanics. Most of the
102 techniques have the limitations of extensive calibration and
103 investigation for their routine use and the production of complex
104 and customarily unclear data. Among these techniques there
105 are some techniques that have contributed significantly to
106 general understanding.

107 Ariola et al. (2) used interfacial rheology for shear (tearing) and
108 dilation (stretching; dilatation) of the interface using a Langmuir
109 trough, and this was considered to provide more of physical but
110 not biochemical description; however, this could depend more on
111 the experimental setup. We might look to undertake such experiments
112 in any enzyme-based future work. Techniques such as surface dilation
113 (21, 22) and surface shear rheology have been used for monitoring
114 protein–protein interactions and Maillard condensation products
115 such as lipid–protein and polysaccharide–protein conjugates (28).
116 Rheology using a Du Noüy ring and Langmuir trough with mathematical
117 fitting has been used for comparable output to our method providing
118 “actual” values. The precise magnitude of these values and their
119 interpretation remain a matter of some speculation, and this was
120 obtained after extensive work. The protein and melanoidin–polysaccharide
121 fraction of coffee was assessed by measurement of interfacial elasticity
122 using oscillatory shear with a Du Noüy ring, and this was related to a
123 kinetic model of network formation (19).
124

125 Our approach is to use the simplest description that might
126 help us resolve small but significant changes in surface composition
127 and could involve pendant polymer chains that dip into the bulk
128 aqueous phase and are associated with a cushion of protective water.
129 In some cases, this might be resolved (in full or in part) by
130 nanorheological means (1, 6) such as atomic force microscopy (AFM),
131 but this is a technique that is difficult to use and is often seen as
132 an expensive and largely inaccessible technique for routine applications.
133 Food apoproteins and lipid

isolated from egg yolk that play a vital role in the use of egg
and its functionality in food were investigated in this manner
(6). Both AFM and Langmuir trough works were used to observe
structure and relate this to interfacial rheology. Two types of
general behavior were observed: aggregates of interfacial material
(measured as a viscous system) and extensive network formation
that may relate to nanoscale aggregations of material but that
clearly exist as a network (measured as a viscoelastic system).
134
135
136
137
138
139
140
141
142

143 In another approach surface rheology was estimated by a capillary
144 wave method that indicated the major difference between surfactant-
145 based (fluid-like) and polymer- or protein-based (highly viscous
146 or rigid-like) interfacial adsorbed layers (17). In both cases the
147 insoluble Gibbs or Langmuir monolayers were dependent on moiety
148 spreading, diffusion to the interface (controlled by bulk concentration),
149 to form a “tough” interfacial film. The properties of casein films
150 were estimated using the additional experimental methods of ellipsometry
151 and X-ray scattering, and this was used to build a picture of
152 interfacial composition (4). Rheological studies here were based on
153 a float but made use of reflected light and a magnet to drive the
154 oscillations that indicate surface properties and provided a “shear
155 elastic constant”, aimed to unravel the determinants of network
156 formation and link this to coarse dispersion stability. In this case
157 evidence of protein multilayers was seen with β -casein at the
158 air–water interface. Surface rheology has also been assessed using
159 an oscillating bubble method (16), but that took 17 h of equilibration
160 and a pendant drop approach (7). These two techniques represent
161 “real food foams and emulsions” in some sense in that they deal
162 with small curved interfaces. Across many considerations, such as
163 ease of use and simplicity of function, they might be seen as less
164 suitable approaches than our equipment for the mass screening of
165 samples but did yield results of high quality. The techniques were
166 used to provide information on the mechanisms of interfacial
167 mechanics, interfacial competition, structuring, synergism,
168 complexation, and binding, and extrapolation to real systems is
169 not always relevant to model systems.
170
171

172 We aim to provide data to support the routine use of a simplified
173 apparatus that performs the same generalized functions as some of
174 the more theoretically oriented methods described above but that
175 can be applied to solutions (and ultimately oil–water interfaces)
176 to provide a more usable form of information but that builds on
177 work already undertaken to allow a fuller understanding of
178 interfacial amphiphile behavior and its ultimate role in determining
179 the quality of foods.
179

180 MATERIALS AND METHODS

181 Solutions were prepared using biological and synthetic pharmaceutical
182 polymers and surfactants (low molecular weight detergents and
183 emulsifiers). Protein samples used included bovine serum albumin
184 (BSA; type A2153 fraction V, purity 96%, lot 26H1013; 67 kDa),
185 human serum albumin (HSA; type A9511, purity 97–99%, lot 24H9314;
186 67 kDa), β -lactoglobulin (BLG; type L0130, purity 90%, lot 033K7003;
187 18.6 kDa), casein (type C7078, lot 100K0223; 24 kDa), and urease
188 type III isolated from jack beans (UJB; type U1500, lot 88H7000; 545
189 kDa), all supplied by the Sigma Chemical Co. (St. Louis, MO).
190 Surfactants used included sodium dodecyl sulfate (SDS; type 166-100,
191 purity >99%, batch 16416; 288 Da) and Tween 20 (T20; product
192 93773; 1.25 kDa) from Fisher (Loughborough, U.K.) and Fluka
193 (Gillingham, U.K.), respectively. Amphiphilic ethylene oxide–propylene
194 oxide copolymer drug delivery pluronics used were F68 NF pastille
195 (Poloxamer 188, Floccor; product G0990395, lot WPYY-647C; 8.4 kDa)
196 and F108 NF prill (Poloxamer 338; product 583062, lot WPMX-543B;
197 14.6 kDa), obtained as a gift from the BASF Corp. (Mount Olive, NJ).
198 All solutions and cleaning were undertaken with surface chemically
198

Table 1. Estimated Air–Water Surface Tensions for a Range of Surface-Active Proteins, Polymers, and Low Molecular Weight Surfactants at pH 7.0 in 50 mM Phosphate Buffer after Equilibration for 10 min at 20 °C

sample	concentration (μM)	CMC (μM)	protein (P), pluronic (X), or surfactant(S)	surface tension ^a (mN/m)
water				73 \pm 1
Tween 20	1	50	S	48 \pm 2 (28)
SDS	1	1000	S	53 \pm 1 (23)
BSA	1		P	58 \pm 1 (52)
BLG	1		P	54 \pm 1 (51)
casein	1		P	58 \pm 2 (50)
F68	1	5	X	52 \pm 2 (40)
F107	1	10	X	53 \pm 2 (40)*

^a Parentheses following the 10 min equilibrium surface tension data for 1 μM solutions indicate the minimum in the surface tension (mN/m) corresponding to a plateau in the tension versus concentration for each amphiphile. * Hydroxypropyl cellulose (HPC) and other derivatized celluloses that are polymers in comparison may give surface tensions of 41–48 mN/m (16).

pure water (surface tension = 72.8 mN/m); all active ingredients were prepared in 50 mM phosphate buffer, pH 7.00, unless otherwise specified. All glassware was cleaned routinely with sulfochromic acid. However, materials that might have been corroded by such cleaning, for example, the conductance electrode and the measuring head device, were cleaned by soft abrasion using a dilute Tween 20 solution, followed by copious rinsing with pure water.

A very limited number of surface rheology experiments involving BSA were undertaken at pH 5.6 in 50 mM citric acid–phosphate buffer to mimic the conditions used for calibration with accrued experimental data (refer to **Table 2**). The materials used in the Max-Planck data were BLG (type L0130, lot 91H7005) and BSA (type A7030, lot 11H0107), supplied by the Sigma Chemical Co., and T20 (Surfact-Amps preparation 10%, type 2830), supplied by Pierce (Rockford, IL).

Foam Stability and Bubble Composition (C_{300}). The technique involving measurement of conductivity was used to probe variations in interfacial composition and to estimate appropriate ratios in binary solution mixtures of polymer and low molecular weight surfactants. The experimental setup is illustrated in **Figure 1**. The configuration is different from previous work, but the principle of operation is well-known and well understood (20–22). Foam stability is defined as the residual conductivity (C_{300}) of an intact foam remaining after 300 s of drainage and the sampled stable thin liquid films (TLFs) (5). Previous work has demonstrated that this approach can be used to map interfacial effects (20, 21) and their extrapolation to the bulk stability (liquid retention) in foams. Because the ionic strength of the buffered solvent is high (50 mM), the technique measures the “volume of entrained liquid” between two electrode wires spaced 5 mm apart but positioned within the body of the foam. Foam drainage shows a typical decay curve (**Figure 1**, panel A). The terminal value after 5 min from the foam column reaching a particular height (23) provides an indication of the residual water held within the foam and can be used to compare samples of pure proteins or mixtures of surface-active agents at a fixed molar ratio (R).

Surface Tension. Samples of 20 mL portions of the liquid tested were allowed to thermally equilibrate for a period of 10 min. A roughened glass microscope slide used for the Wilhelmy plate ($2 \times 2 \times 0.02$ cm) method was used to determine the interfacial composition and surface tension (mN/m) using a torsion balance and the appropriate weight of detachment from the air–water interface. Pure water was found to have a value of 72.8 mN/m at 20 °C (21, 22).

Interfacial Shear Rheology. The basis of the experimental technique is the damped oscillation of a pendulum after an initial fixed deformation (**Figure 2a**, lever position A to B). The number of swinging pendulum oscillations is related to the viscoelastic properties of the adsorbed surface layer (24) (when other contributions are neglected) situated in the plane of the interface. Ultimately, the pendulum stops to oscillate, and this is directly related to a surface damping effect on the measuring head over and above that of the bulk aqueous phase or surrounding

air. In its simplest format the apparatus consists of a steel torsion wire, a measuring head (bob), a trigger switch, and the sample solution (**Figure 2a**, panel A). The dimensions of the apparatus and spatial alignment are fixed so that there is equal treatment between samples.

Initial calibration of the pendulum was undertaken in air and water, providing 292% damping of the number of oscillations in air. All sample measurements were blanked against the damping found for a fresh interface formed on a pure sample of water (surface tension = 72.8 mN/m at 20 °C). In our experimental configuration the 69.2 g magnesium–aluminum alloy, 61.8 mm diameter measuring head (and fixings), and 69.5 mm long copper trigger (**Figure 2a**) dimensions and the bob interfacial immersion are fixed and safeguarded against air movement or other interferences by housing in a protective sheath. The trigger is responsible for completing an electrical circuit (**Figure 2b**) indicated by both a red diode output and recorder square-wave signal (**Figure 2b**, panel B). The number of contacts and hence square-wave signal peaks can be counted (or the entire span measured and thus equated to a number) and related to a surface damping when related to those seen with water. The point when the trigger fails to make contact with the trigger plate, even though the measuring head may still be oscillating, corresponds to the end of the experimental data acquisition for every sample solution.

The standard concentration used was 1.0 μM in studies involving proteins; other concentrations tested are indicated at the appropriate point. Measurements are made by placing 35.0 mL of test solution into a cleaned 9.6 cm diameter, 1.0 cm deep glass dish. The sample was left to surface and thermally equilibrate for at least 2 min, but as a matter of routine and standard practice, for 20 min. Measurements follow an initial 15° deformation of the position of the bob sitting on the surface of the test sample. Measurements were usually related to triplicate repeat runs all undertaken on the same sample. For the purposes of relating damping to estimates of surface viscosity (15), previously unpublished data and sample mixtures used for testing of a new apparatus were used in this study. The vertical location of the measuring head is such that there is no effective immersion into the bulk phase, but the contact angle of the meniscus of the solvent with the sidewall of the bob is very small and close to 0°. The vertical “z” and lateral “x–y” positioning of both the sample dish and the trigger contact post (made from brushed copper tubing) were achieved using a mechanical lift.

RESULTS AND DISCUSSION

The properties of macroscopic interfaces are thought to represent effective models of the interfacial adsorbed layer of foams and emulsions. **Figure 3** (panel A) shows the difference in initial foam drainage form and rates between foams that are stabilized by proteins and surfactant, respectively. Interfacial adsorption and rheology using a pendant drop model (7) have been used to investigate protein–protein interactions that are relevant to food and dispersion form. It is reportedly the “depth” of these interactions that promotes bubble stability (7, 22). With protein-stabilized foams the thin liquid films (TLFs) separating the bubbles are thicker, and consequently entrained liquid and thus microconductivity values (μS) at the same moment in time are higher than with simple surfactant such as SDS. Even after 5 min of drainage, there is more water within a BSA-stabilized foam as compared to an SDS-stabilized foam, despite the bubble size being approximately the same (2 mm diameter). This is thought to be related to the pendant chains of polymer/protein that protrude away from the bubble surface (3, 9, 13, 19, 21, 22, 26).

Foams and their foam lamellae are used to assess the concentrations that relate to fragmentation of the interface on TLFs (5, 13) and foam bubbles (21). At very low molar ratios the adsorbed layer immobilized at the interface is thought to effectively fragment, and this has formed the bases of considerable previous study. The mechanism behind the dissolution of protein–protein interaction as in protein-stabilized foams is thought to be the competitive adsorption of surfactant (6, 20, 21).

Table 2. Estimated Air–Water Surface Viscosity [Data in Parentheses Represent First the Surface Viscosity at 6 min and Second the Surface Elasticity ($\mu\text{Pa}\cdot\text{M}$), Supplied for Reference Only] at 10 min at 20 °C and Apparent Pseudo-Equilibrium Conditions versus Measured Percentage Damping That Forms the Calibration To Estimate Surface Viscosity^a

sample	concentration (μM)	projected (MPI) surface viscosity ^b ($\mu\text{Ns/m}$)	% damping (UoB) ^c
β -lactoglobulin (BLG)	1.0	3800 (3028, 0.0)	12.54 \pm 0.6
Tween 20 (T20)/BLG molar ratio, $R = 0.09$	BLG fixed at 1.0	3700 (3493, 0.0)	10.03 \pm 0.4
T20/BLG molar ratio, $R = 1000^d$	BLG fixed at 0.1	70 (10.9, 2.7)	1.67 \pm 0.1
T20/BSA, pH 5.6, molar ratio, $R = 0.05$	BSA fixed at 1.0	3480 (3085, 0.0)	15.42 \pm 0.2

^a The projected data are based on fitting and extrapolation of the form of actual experimental data ($R^2 = 0.9\text{--}1.0$). The bulk protein concentration of solutions tested is 1 μM except where otherwise specified, and solutions were all made in 50 mM sodium phosphate buffer adjusted to pH 7.00 except where otherwise specified, in this case 50 mM citric acid–sodium phosphate buffer was used. ^b MPI refers to the Max Planck Institut; data collected in the past but not presented, see ref 15 for experimental setup. Extrapolated from data taken at 120–240 s showing a standard deviation of approximately 6%. ^c UoB refers to the University of Brighton equipment. ^d Relates to a system that is dominated by the nonionic surfactant (because of the reduced protein concentration and Tween presence in excess) and in some sense can be “taken to represent” the surface on a Tween/low molecular weight only solution, according to previous foam stability work (20–22, 24, 25).

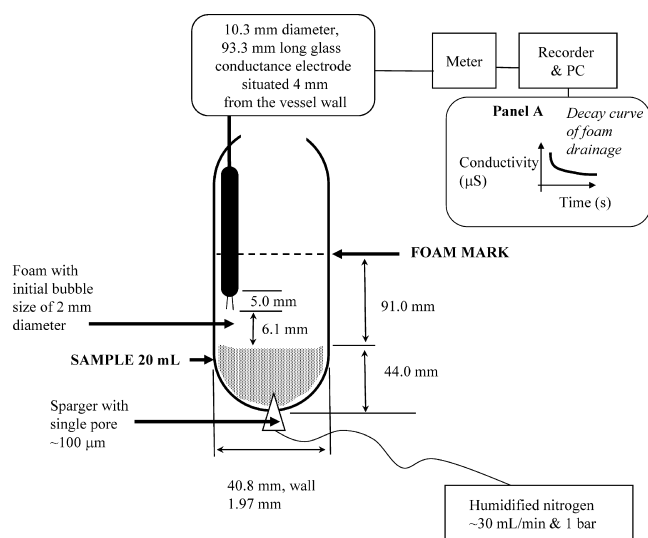


Figure 1. Schematic representation of a basic foam stability apparatus used for selection of appropriate mixtures of surfactants and proteins and in some cases polymers (20). Microconductivity gives an estimate of the water entrained in the foam during foam drainage. It can also give an insight into other processes such as bubble rupture and coalescence and indirectly point to interfacial composition. The apparatus in standard format uses 50 mM phosphate buffer at pH 7.0 to over-ride the contributions of the surface active molecules and thereby measure water content. Panel A shows a typical decay curve that is seen with time. The conductivity remaining in the foam after 5 min of drainage is taken to represent a measure of foam stability (C_{300}); measurements are undertaken at 20 °C.

This has also been shown to be true for poly(ethylene oxide) polymers and SDS (10).

Panel B within the **Figure 3** shows the familiar foam stability curves for binary mixtures of protein and surfactant (21, 24); the graph can be explained by the alteration in the surface composition following competitive adsorption of surfactant over protein or, in some cases, interfacial replacement. Interfaces that contain less polymer stabilizer tend to give thinner TLFs. As the dissolution of interfacial cross-links between adjacent protein (polymer) molecules is increased within the foam, it becomes more unstable and susceptible to bubble coalescence. This has been studied in detail for food foams and a number of simple model systems (20). The molar ratio (R) at which significant dissolution appears is usually considerably less than 1.0. In previous work this has been found to occur at $R = 0.1$ in dilatational rheology (21), $R = 0.25$ (22), and $R = 0.33$ (25), all of which depend on the protein species and its inclination to stay at the interface and the type of surfactant present. In the

protein–surfactant mixtures tested with interfacial rheology here, values of $R < 0.1$ were used, and these correspond to the initial dissolution of intermolecular cross-links. At very high molar ratios the interface resembles a composition that is similar to that formed from a pure surfactant solution (**Figure 3**, panel B).

Small molecular weight surfactants tend to dominate at the interface when in competition with proteins and polymers. **Table 1** shows the surface tensions of dilute solutions and those at plateau equilibrium concentration (minimum in surface tension). Proteins (BSA, BLG, casein mixtures) generally give surface tensions in the region of 50 mN/m; effective polymeric emulsifiers were found to give equilibrium surface tensions of 40 mN/m, but smaller surfactants are able to significantly reduce the air–water surface tension to <30 mN/m. Given a mixture of BLG and Tween 20, the surfactant or a complex of protein and surfactant (22) has been shown to predominate over the native protein molecule. Previous work has shown that polymers can displace protein from the interface (24), and some studies (16) report on cellulose derivatives having surface tensions of about 45 mN/m. This could be of significance when food gums and proteins are combined in processed foods and a likely subject of future work.

A series of solutions of surface-active molecules were tested for their ability to damp the movements of a probing surface shear device. The results are presented in **Figure 4**; here the effect of equilibration time was demonstrated clearly. In previous theoretical work equilibration times of 12 and 17 h have been considered before equilibrium conditions were achieved. These techniques generally used very large volumes and very dilute solutions (16, 27). One of our primary aims has been to reduce the length of time taken before measurement, and for this reason we do not look to directly measure surface viscosity.

Rheology in various forms can thus be used to test covalent linkages. At present a scientific fixation with absolute measurements (viscoelasticity models; G^* , G' , and G'') means the techniques are overly complicated and not used for effective rapid screening of possible formulation candidates as we suggest (27). In the methodologies mentioned by these authors and others, equilibration of the sample took more than half a day for pseudo-equilibrium conditions to be obtained and used up to a quarter of a liter, almost 8 times the volume we use. Because the behavior is very typically “nonlinear”, the surface shear viscosity (stress/strain; η_s) and its development depend on many variables associated with the experimental data acquisition and the way it is physically sampled; this can ultimately provide difficulties in cross-comparing samples. This is made even more complex when extracted values such as G' and G'' are extracted from derived mechanical spectra (19).

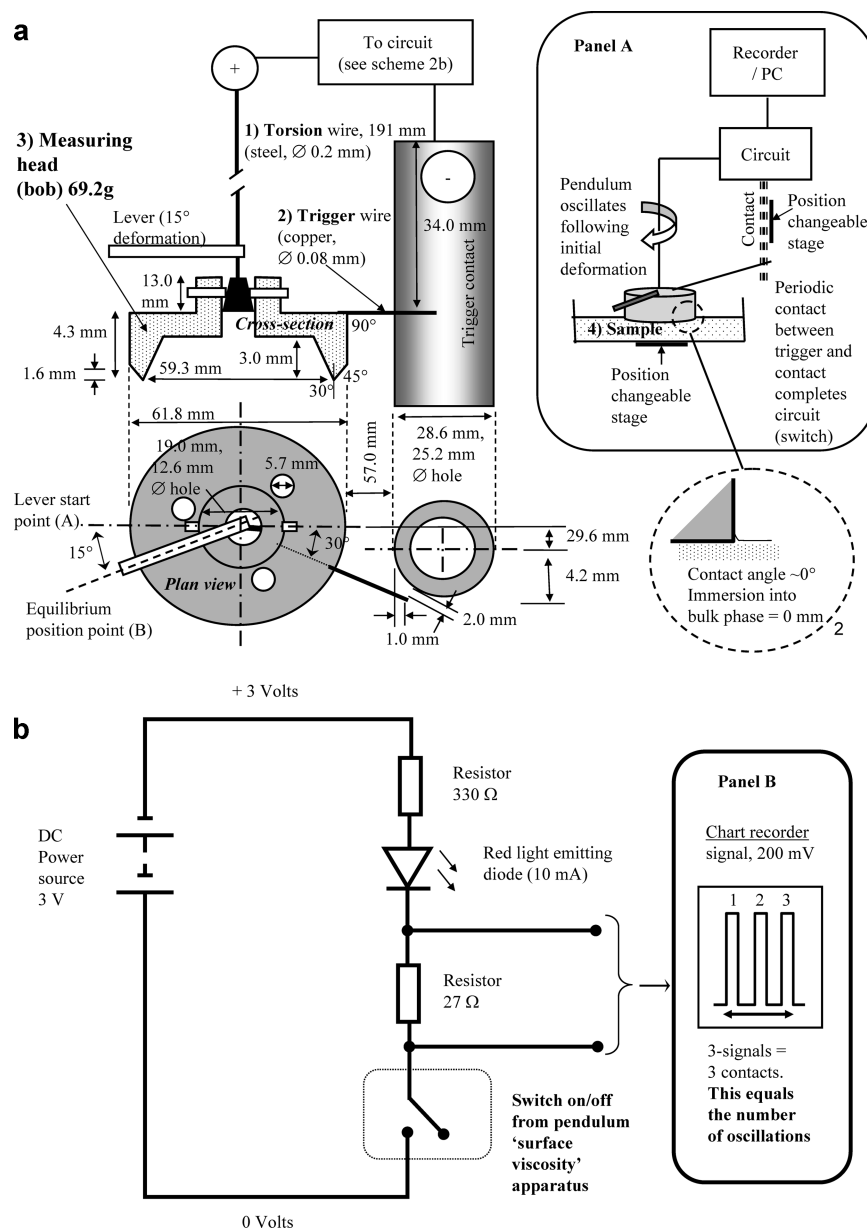


Figure 2. Schematic representation of the experimental setup of an air–water surface rheometer. (a) shows the basic components of the instrument: (1) torsion wire, (2) trigger mechanism, (3) measuring head; panel A indicates the fourth major component, which is (4) the sample itself. Within a, panel A shows in the simplest form the basic mechanism of measurement. The pendulum with measuring head fixed on the end has its movement initiated by the lever being released from starting position A to position B. (b) shows a simple representation of the “switch” and acquisition of a square-wave signal based on the number of contacts between the trigger wire and the trigger contact. Damping due to the properties of the interface represents one of a number of contributions to a slowing of the measuring head oscillations. Measurements were undertaken at 20 °C.

383 According to **Figure 4** low molecular surfactants do not
 384 appear to give a significantly more rigid interface when left to
 385 surface equilibrate for up to 20 min. With BSA alone and BLG
 386 protein in the presence of Tween 20 ($R = 1000$), the percentage
 387 damping increased with equilibration time. This in principle
 388 corresponds to a stiffening or thickening in consistency of the
 389 adsorbed layer, but may also reflect a transition from “elastic”
 390 to more “viscous” surface-aggregated (2, 7, 27) adsorbed
 391 interfacial material. This was observed in previous studies using
 392 bifunctional agents (22, 25) and seen on the aging of the
 393 interface that relates to molecular “juggling” and position
 394 optimization at the interface (14).

395 However, with casein and BLG protein in the presence of
 396 Tween 20 ($R = 0.09$) the surface damping decreased with
 397 equilibration time. In the case of the latter this may be due to

398 significant rearrangement and dissolution of protein–protein
 399 interactions. Recent investigations show that aging (14), with
 400 respect to development of significant viscoelasticity, occurs at
 401 the interface with proteins. This is explained in terms of the
 402 moiety hydrophobicity and the extent of flexibility in the
 403 molecule that permit the ease of reformation at the interface,
 404 alongside its neighboring molecules that leads to an increase in
 405 surface rigidity. This is particularly thought to be the case with
 406 many foods for which the textural “elastic form” of material
 407 surrounding gas bubbles or fat crystals is an important indicator
 408 of quality, such as bread dough and in cakes and pastries.

409 With casein samples, although the percentage of surface
 410 damping decreases between 2 and 90 min, the effect was
 411 marginal, and it is difficult to say whether this is a real effect
 412 or simply due to experimental variation. Our sample was a

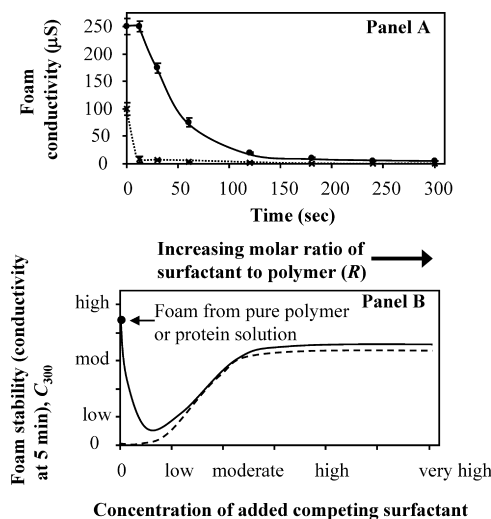


Figure 3. Panel A shows foam drainage data for 0.8 mg/mL solution of BSA (12 μM) pH 7 (●) and 3.5 mM SDS at pH 7 (×) at 20 °C in 50 mM sodium phosphate buffer. Panel B provides an example of typical foam stability curves for low molecular weight surfactant (broken line) a fixed concentration of protein (●) and a fixed concentration of protein/polymer in the presence of increasing low molecular weight surfactant (see refs 21 and 22) indicated by the continuous line. The foaming apparatus can provide information on the point at which a protein-stabilized foam interfacial adsorbed layer begins to be affected by inclusion of a competing surfactant. This was the basis of the mixtures used in rheological studies. The experimental conditions are as indicated above.

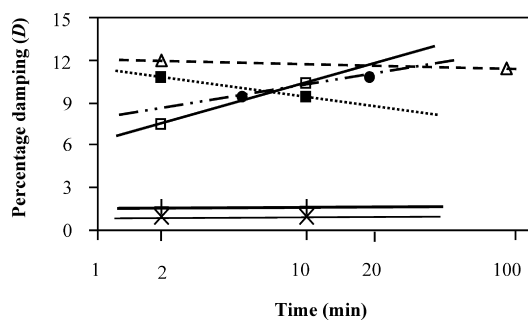


Figure 4. Plot showing the changes in surface "stiffness" and percentage damping of a measuring head (D) located in the plane of the adsorbed air-water interfacial layer against equilibration time for solutions in 50 mM sodium phosphate buffer at 20 °C. The samples represented are 1 μM BSA (●), Tween 20/BLG mixtures with 1 μM BLG at a ratio, $R = 0.09$ (■), Tween 20/BLG mixtures with 1 μM BLG at a ratio, $R = 1000$ (□), 13 μM casein (Δ), 300 μM anionic SDS alone (\times), and 100 μM nonionic Tween 20 alone (+). Experimental error in the percentage damping values for each of the samples ($n = 3$) is in the range of 6–7%.

mixture of caseins (α_{s1} , β , κ , etc.), and recent work (4) have shown that the association between α_{s1} and β (>50% of protein fraction) caseins is primarily responsible for surface viscoelasticity and product functionality in solution or at the interface. In any case, the magnitude of change was negligible, and we suppose that a form of pseudoequilibrium of the interface can be assumed to take place within 20 min given the small volume of sample needed with our apparatus. Given that the equipment's principal purpose is to compare samples, most measurements were taken after 20 min of thermal equilibration.

The percentage damping that is synonymous with surface consistency increases (D) appears as four forms in **Figure 5**. Water and low molecular weight surfactants appear to give

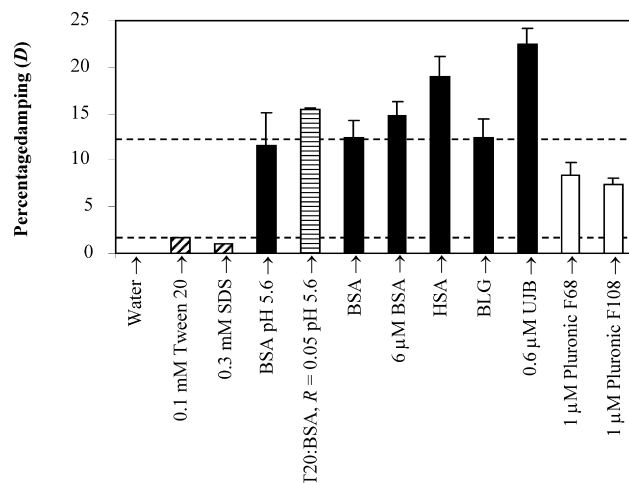


Figure 5. Plot showing the percentage damping of a measuring head (D) located in the plane of the adsorbed air-water interfacial layer after 20 min of equilibration time for various sample solutions in 50 mM buffer at 20 °C. The samples represented are proteins (black bars), polymer (white bars), mixed protein-Tween (T20) (horizontally shaded blocks), and surfactant (diagonally shaded blocks). Protein concentrations are 1 μM , and the pH of solutions is set at 7.0 except where otherwise stated. BSA samples adjusted to pH 5.6 used 50 mM citric acid-sodium phosphate buffer. The broken lines indicate the values found for BLG representing a strongly viscoelastic surface and that for Tween 20 representing a poorly viscoelastic surface (22). The samples noted as abbreviations are sodium lauryl sulfate (SDS), bovine serum albumin (BSA), human serum albumin (HSA), jack bean urease (UJB), and β -lactoglobulin (BLG). The measurements are based on three or more replicates.

values between 0 and ~2%, respectively. Interfaces stabilized by protein and a mixture of protein with some incorporated surfactant give much higher values between 12 and 23%, and surface-active polymers (such as poloxamers) give values between 7 and 9%. β -Lactoglobulin that has been studied extensively in terms of dilatational rheology and development of significant surface "elasticity" (21, 22, 25), and constant shear viscometry at the oil-water interface (23) gives a surface damping value of 12.5% and is indicated by the broken line in the figure. Depending on the technique used, this protein is thought to give highly viscoelastic adsorbed layers (21). These are often considered to be in the form of multilayers that are based on a cohesive single primary adsorbed layer of protein molecules (2, 27).

The interplay of food ingredients in a real system such as coffee foam was used to investigate protein-carbohydrate complexes (19). Interfacial effects were considered to be due to the interaction between the lysine amino groups of the protein fraction and carbohydrate ester groups. Other nonspecific molecular interactions in the interfacial layer were thought to be related principally to electrostatic and hydrophobic interactions. The group noted the findings of interfacial measurements, and these correlated well with foam stability as in our case. When the interface is considered to have a significantly high damping value, this correlated well with the C_{300} values (**Figure 3**) that are higher for BSA than for simple surfactants, such as SDS, that demonstrate weak damping (**Figure 5**), and this is associated with water retention in the TLF subphase in the foam associated with the interfacial presence of hydrophilic polymer (3, 26) as found with colloidal particles.

Two of the proteins examined are distinguished from what might be considered to be conventional model globular proteins

(BLG and BSA) under a range of conditions that have a D value of 12–15%. In the case of human serum albumin (HSA) this damping is increased by approximately 150% from that measured for BLG, and in the case of jack bean urease (UJB) this value is 180% higher. Both HSA and BSA have the same molecular weight, which is approximately 3.5 times that of BLG, and so it can only be assumed to be related to the extent of interfacial cross-linking that depends on the small-scale molecular differences between BSA and HSA, possibly in the location and number of hydrophobic, charged amino acids, or disulfide bond content (11). In the case of UJB the protein has a molecular weight >29 times that of BLG, and this may explain the scope for greater interfacial cross-linking (2, 14) and entanglement and the subsequent increase in the rigidity and damping of the interfacial layer.

The pluronic samples measured have marginally different molecular weights but seem to contradict this molecular weight related “viscosity” increase. Here, the 14.6 kDa F108 has a lower interfacial viscoelasticity than the F68 species, which is 42% smaller and yet present at the same molar concentration. This could be related to the time of pseudoequilibrium rearrangement, local interfacial conditions (26), diffusion to the interface, and coverage of the surface (3, 9, 1018). The smaller species should diffuse more rapidly and may take less time to unfold or reorient at the interface. In either case, it is noteworthy that the D values for these pluronics (poloxamers) are 40% less than seen with BLG (but ~500% more than with Tween 20). This is obviously related to the diversity of potential cross-links with the BLG overly simple block copolymers such as poloxamers and, thus, margin for development of greater interfacial “viscoelasticity.”

The damping (viscosity, as measured here) is a function of the inertia of the bob suspended as a pendulum and its interaction with both the circuit trigger (via a hair-like spring) and primarily the interfacial adsorbed layer, elasticity in the wire, and a damping provided by both the resistance of the air and viscous drag from the water or other primary solvent used on which the bob rests. The best and most convenient description is explained below as a simplified function with multiple contributions; each of the contributions can have a range of domain values.

$$\text{surface damping parameter } (d) = f(I, E, s, P, W, a) \quad (1)$$

Elemental contributions are indicated as I , inertia following the 15° initial swing of the pendulum bob; E , elasticity of the 200 μm diameter, 191 mm long steel wire; s , elasticity and spring-like damping from the 80 μm diameter copper wire trigger; P , damping resulting from the surface molecular layer; W , damping resulting from the interfacial subphase; and a , damping resulting from the air surrounding the pendulum bob. Major contributions are presented in capital letters, but in our highly standardized model equipment only the damping of the interfacial layer is allowed to vary between experimental runs.

The 69.5 mm copper trigger hair has a $13 \pm 3\%$ contribution to the normal damping of the pendulum in air (150 ± 2 full swings); this can be seen as a 5% decrease in the number of swings in a minute when the contact with the trigger contact (Figure 2a) is removed. In any case this is a point of limited further detailed discussion because the equipment was always run with the contact possible for all of our measurements. The contact is needed after all to complete the circuit. What dictates the contact made is the number and extent of swings in the oscillations of the measuring head (bob). These oscillations are directly influenced by interaction between the device measuring

head and molecules located in the plane of the interface. In this manner the technique is superior in many ways to optical-based techniques such as pendant drop or bubble form methods in that a direct physical sampling of the interface takes place and, second, in that the shear rate of the bob is reduced (and thus sensitivity is increased) by this interaction on each marginally less pronounced successive pendulum swing.

The real “apparent” surface viscosity can be estimated with the use of calibration studies. The value of this lies in simply being able to describe events occurring at the surface in another way. These calibration data and experiments were previously performed during collaborative investigations (15). Using a simple fitting program, these can be approximated to our findings with a four-point calibration (see Table 2) to give predicted viscosities ($\mu\text{Ns/m}$) and are described in a minimized form in the following highly simplified relationship ($R^2 = 0.949$, $n = 4$):

$$\text{apparent “predicted” surface viscosity } (\eta_p) = [k_1(\ln D)] - k_2 \quad (2)$$

k_1 is a constant of 1719, D is the percentage damping of the sample, as the surface damping parameter (d) compared to that seen with a clean interface from pure water, and k_2 is a constant of 713.

The constants in this case are dimensionless values and simply scale the viscosity against the percentage damping. The first point worth noting is the good fit between extrapolated surface viscosity and damping described above. The apparent viscosities are based on an extrapolated value after 10 min (η_e) with a correlation coefficient close to 1.0 for each of the values shown in Table 2 and incorporated into the testing regime, based on real experimental data acquired up to 6 min (15). In our case fuller equilibration time is always taken as 20 min (at least 10 min), even though preliminary experiments (Figure 3; Table 2) indicate that the equilibration time, particularly for polymer-stabilized interfaces, takes longer than the 2–6 min to reach plateau pseudo-equilibrium values. The more “retarding” the interaction between the metal bob (measuring head) and the surface the higher is the percentage damping. As can be seen from Figure 4 the damping for a solution of 0.02 mg/mL (1 μM) BLG is about 12.5% (Table 2, about 10 times greater than that seen with a submolar surfactant solution interface (Figure 5).

In our system we are unable at present to disaggregate the “elastic and viscous” components of the measured damping parameter. However, this might be undertaken as part of future studies, but we do not consider this to be as important as the ability to compare samples for future envisaged evaluation. What is clear from our data is that the elasticity is customarily lower when the viscosity is higher (compare values in parentheses in Table 2, for protein mixtures); very low elasticities are to some extent “inventions”, possibly created by inappropriately “timed” evaluation of Gibbs-type surfactant monolayers or mathematical dissection of raw data. Similarly, the technique described here measures percentage damping, and although it is clear that there is some effect for simple surfactants, the values are surprisingly high when compared to known “viscoelastic” protein-based interfaces such as that formed from BLG or BSA solutions (~14% of the value for BLG alone). This is repeatedly observed for the measured damping for Tween 20 and SDS interfaces, which are essentially “fluid-like” but provide a definite positive D value (Figure 4) when compared to a fresh interface formed on water. It may also suggest that our technique is able to “see” very low surface viscosities. The other real value of the novel

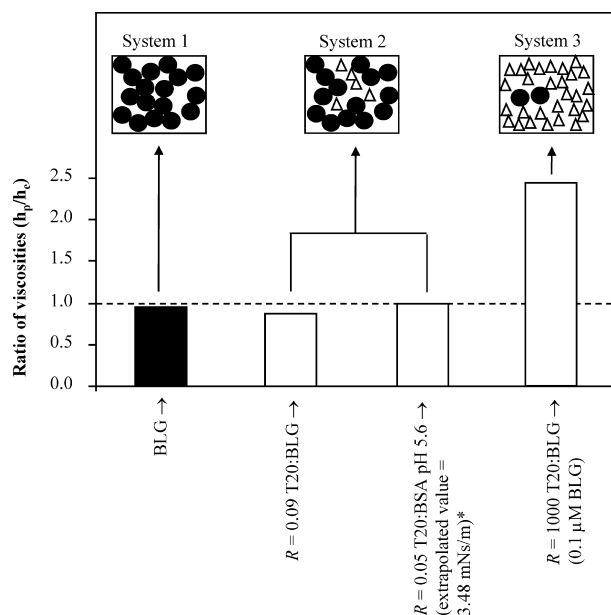


Figure 6. Plot showing the ratio-fitted predicted viscosity (η_p) to actual experimental (projected) viscosity (η_e) as indicated in **Table 2** and conditions given therein using a measuring bob located in the plane of the adsorbed air–water interfacial layer. The fitted data (η_p) relate to measurements after 20 min of equilibration time for various sample solutions in 50 mM buffer at 20 °C. The actual data (η_e) represent extrapolation of the viscoelastic properties of identical solution surfaces from data obtained between 2 and 6 min of equilibration to 10 min. In both cases the geometries of the measuring devices used for surface rheology were similar but not identical. The samples represented are proteins (black bar) and mixtures of protein with Tween (T20) (white bars). Protein concentrations are 1 μ M, and the pH of solutions is set at 7.0 except where otherwise stated. BSA samples adjusted to pH 5.6 used citric acid–sodium phosphate buffer. The broken line indicates a ratio value of 1.00. An experimentally determined viscosity value for T20/BSA mixtures is indicated (*) for reference. The plot demonstrates that the predicted and actual extrapolated values are often in very close agreement. The measurements from a fitting procedure represented are based on three or more replicates (experimental variation in values determined is set at approximately 10% in total). The figure also shows a phenomenological interpretation of interfacial composition; three scenarios are considered (referred to as systems 1, 2, and 3). In the model low molecular weight surfactant molecules (Δ) and polymer or protein molecules or nanoscale aggregates of proteins (\bullet) that are adsorbed at the interface are shown (not drawn to scale).

apparatus lies in its ability to clearly discriminate and quantify the resistance offered to the metal measuring head. Previous studies have indicated that foam and emulsion thin liquid film form, based on surface adsorbed material is responsible for conferring stability properties on coarse dispersions (19, 2122).

Using the estimation it seems that there is a considerably good fitting between the predicted surface viscosity (eq 2, η_p) and the projection of experimentally monitored viscosities. This can be demonstrated by reference to the ratios presented in **Figure 6**. Here, a ratio of 1.0 indicates that the predicted “surface viscosity” is identical to that of the model data (extrapolated 10 min data) on the basis of results from experiments undertaken at the MPI.

With β -lactoglobulin-stabilized systems the effect of time on spreading of the protein at the interface is of significant interest and extensive contemporary debate. In “pure” protein systems (solutions) this time-related surface equilibrium is considered

to be extensive; however, for mixtures (particularly lipids or surfactants) this equilibrium is generally much shorter, and this can be a consequence of rapid bulk-surface diffusion and the effective competitive adsorption of low molecular weight amphiphiles over polymers. From a range of observations and ancillary measurements (not reported), it appears that globular particles adsorb and then reconfigure slowly over a period of many minutes to hours to form a spreading microheterogeneous mass. This observation is supported by a considerable body of scientific data, including neutron reflectance and atomic force microscopy measurements (6) and many other experimental delineatory approaches. The form of this cross-linked mass is at present not entirely clear, although current thinking points to an aggregate-cross-linked monolayer. There is an equilibrium established between this spreading and the arrival of “new” and the departure of “old” molecules with respect to the interface. Additionally, the way lactoglobulin interacts at the oil/water (O/W) or air/water (A/W) interface is likely to differ significantly from that of nonglobular proteins, such as caseins, or that of the very bulky and rigid globular proteins, such as BSA. The basis of these differences may be related to molecular shape, portion polarity, and molecular rigidity. These differences are likely to affect the surface conformation of the protein and thus its surface damping properties, and also its bulk properties such as viscosity or its ability to form a gel. There is also likely to be “some” difference between the behavior of polymeric amphiphiles at O/W and A/W interfaces, and this has been widely reported over the past two decades.

Four systems were used to compare and in some way give an estimate of a “real” surface viscosity. These were protein alone and three various mixtures of Tween 20 with proteins. The ratio (**Figure 6**) is very close to 1.0 for both BLG and $R = 0.05$ Tween with BSA systems and slightly less so for the $R = 0.09$ Tween with BLG system (minus 10%). These ratios were selected because they correspond to the decrease in foam stability on inclusion of competing surfactant discussed at length previously (18, 21, 22, 25). In this way they were considered to be appropriate models for the change from polymer- to mainly surfactant-stabilized interfaces and interesting candidate systems for interfacial modeling.

The fourth piece of data, for diluted BLG and excess Tween 20 ($R = 1000$), does not match as closely to the extrapolated experimental values of 0.070 mNs/m at 0.17 mNs/m and is observed on the plot at a ratio of 2.4. This is still substantially lower than the ~ 3.7 mNs/m viscosity values seen with the proteins tested. It seems that the technique is less substantive for prediction of very low “viscosities” than seen with polymeric systems such as protein-stabilized interfaces. Nevertheless, the technique we use is able to clearly distinguish the properties of a “fluid” (simple surfactant) interface from those of a more rigid (protein) interface, and to this extent the simple and easily applied, rapid technique serves a particular purpose for the examination of foods and pharmaceutical polymer mixtures.

Figure 6 also shows a cartoon for each of the three distinct types of surfaces thought to exist in the solutions examined. System 1 is an interconnected interfacial layer, showing considerable lateral cohesion, and is thought to exist as a series of interconnected polymer molecules or interconnected aggregates of polymer molecules. This type of system is thought to exhibit considerable levels of viscoelasticity and is envisaged to be present with polymer-only systems or where the level of competing surfactant is too low to have a measurable interfacial impact. System 2 is similar to system 1, but in the former, intermolecular or interaggregate cross-links and connections start

664 to be lost by positioning of intervening surfactant molecules (13, 19).
 665 In this case, an increased interfacial viscosity may be measured
 666 at the expense of the “elastic” and rigid nature of the interfacial
 667 layer. This was certainly observed for BLG in the presence of
 668 lecithin (LPC)-based surfactants using surface dilatational
 669 elasticity measurements (21). The third scenario, with an excess
 670 of surfactant, resembles the interface in the presence of
 671 surfactant alone (with minimal levels of protein inclusion that
 672 may or may not have much impact). Here, lateral interactions
 673 between adjacent surfactant molecules are weak when compared
 674 to those found between proteins, and the interfacial viscoelas-
 675 ticity is low. The second scenario is expected for surfactant–protein
 676 molar ratios (R) of less than, for example, 0.1 but unlikely to
 677 exist at $R = 1000$. At such high surfactant concentrations the
 678 interfacial layer is fluid and exemplified by our system 3. It is
 679 likely that intermediary combinations of all three systems also
 680 exist, but this would depend on the protein, its interfacial
 681 concentration, and its scope for interfacial desorption and
 682 intermolecular cross-linking (4, 14, 27, 28).

683 An important consideration in the pragmatic use of the results
 684 of the rheometer is to assess their value with respect to food
 685 and other complex bionanotechnologically related systems (13).
 686 In this case, unlike the “model and simplified” systems often
 687 described in this paper and the macroscopic planar interfaces
 688 examined, there may be interaction between the interfacially
 689 adsorbed material and material contained within the bulk phase
 690 or entrained liquid that is found within a foam or emulsion
 691 lamella. The latter is a common occurrence in protein-stabilized
 692 emulsions and foams, particularly with multiphase media such
 693 as foods in which there is undoubtedly an interaction between
 694 adsorbed layers and polymer, lipid micelles, ice, or other
 695 aggregates and crystals (6) that constitute or form part of the
 696 dispersion phase. Such interactions are likely to strongly affect
 697 damping; however, by using suitable experimental reference
 698 environments (solutions) under which this additive behavior is
 699 not so pronounced, it may be possible to elaborate further on
 700 the mechanisms involved and indicate the extent of such
 701 interactions and their relative predominance over the measured
 702 effects of the surface adsorbed layer itself. We believe our
 703 approach is powerful in that it should enable the user to measure
 704 such phenomena, but it will be difficult and challenging to
 705 directly disaggregate the individual elements of the measured
 706 damping and identify the exact source of this damping directly
 707 from the data. Typically, in such a case when the bulk viscosity
 708 (consistency; viscoelasticity) and its intrinsic contribution to
 709 damping are very high, suitable adjustment may be required or
 710 may not be possible. Our aim is to test these possibilities in
 711 future work when we progress from simpler systems to more
 712 realistic models of “liquid-like” food and pharmaceutical/
 713 nutraceutical dispersions.

714 In experimentally tested (more dilute) solutions, this bulk
 715 phase enhancement of measured damping contribution over that
 716 of the continuous water phase (taken as a control) is negligible,
 717 yet interestingly, it may be possible using suitable time-related
 718 calibration studies to get a “scaling” of the depth of this
 719 interaction. There is strong experimental evidence to suggest
 720 that both thixotropy and rheopexy within the measured surface
 721 layer (and subphase) and development of molecular associations
 722 and entanglements are time-related events (14). When these
 723 types of concentration regimens are used and the likely
 724 magnitude of effects seen with highly viscous bulk phases is
 725 considered, judgment of this influence over the total measured
 726 damping will take a more pragmatic delineatory approach. It
 727 is, however, the case that the pendulum device bob and its

728 vertically tapered “sharp” edge are purposely in contact with
 729 the smallest portion of the bulk phase, and thus bulk phase
 730 damping tends to minimize given this geometry. At present we
 731 have not looked at “solutions or slurries” with this degree of
 732 extensive contribution to measured damping, and accordingly
 733 at the relevant point some appropriate alterations and a
 734 modification to the equipment methodology may be considered.

735 The foaming apparatus and its ability to predict or reflect
 736 interfacial composition is now reasonably well understood (7).
 737 Its value lies in providing an additional picture when combined
 738 with tensiometry to more fully describe various interfacial
 739 structures and their influence on the gross properties of food
 740 and other industrial preparations. The composition has an
 741 undisputed impact on the physical texture and mouthfeel and
 742 visual assessment of shelf life and in some cases on the chemical
 743 shelf life of food products by permitting incorporation, seques-
 744 tration, or exclusion of preservatives (12) or degradation
 745 products (19, 28).

746 There are some drawbacks associated with this new rheo-
 747 logical equipment, which include its oversimplification, modular
 748 composition, and rapid nature of measurement. For many
 749 experienced rheologists this oversimplification presents itself
 750 as providing little theoretical information that might be inap-
 751 propriately judged to reveal little value in the approach. We
 752 find the technique more valuable because it generates a
 753 numerical index with which to compare samples rather simply
 754 generating elasticity or viscosity values that are obtained from
 755 mathematical dissection of an output signal (27). In the case of
 756 complex samples this transition between mainly viscous, mainly
 757 elastic, and weakly viscoelastic interfaces presents problems in
 758 terms of trying to create a simple rationale or replicating
 759 experimental conditions for selection of an appropriate mix of
 760 ingredients and can be subject to small changes in pH, ionic
 761 strength, or temperature, which lead to differing extents of
 762 aggregation of polymers with time (14). The technique should
 763 be of considerable use to those scientists requiring a simplified
 764 picture of the interfacial loading of materials and a reflection
 765 of interfacial composition as a route to greater understanding
 766 of real food products rather than theoretical work with highly
 767 purified food-grade proteins, emulsifiers, and texturizing polysac-
 768 charide gums and synthetic polymers. One of our future aims
 769 is to test the device on real liquid samples such as beer and
 770 milk. The second is to be able to resolve the makeup of solutions
 771 following the dissolution of mixtures of powdered ingredients,
 772 and the third could involve assessment of the influence of the
 773 presence of naturally occurring functionality boosting agents.

774 In conclusion, the interfacial rheometer is used to assess the
 775 damping of adsorbed layers assembled on aqueous solvents.
 776 Polymers appear to produce much greater surface damping than
 777 simple surfactants. The extension of our work is to use the
 778 rheology apparatus to comparatively probe the synergistic or
 779 antagonistic effects seen when binary or more complex mixtures
 780 of surface-active ingredients are used. Further work might
 781 include the actual determination of elastic and viscous elements
 782 of the determined surface damping parameter. Although the
 783 precise value of this complex information for routine assessment
 784 of food mixtures is not clear, the rheometer mentioned here is
 785 robust and simple and provides enough detail to be able to test
 786 different samples of food ingredients.

787 ACKNOWLEDGMENT

788 D.K.S. thanks Drs. Jürgen Krägel and Reinhard Miller,
 789 formerly at the Max-Planck Institut für Grenzflächenforschung

790 (MPI), Berlin, for the use (and unpublished data obtained) of a
791 developmental interfacial rheometer.

792 LITERATURE CITED

- 793 (1) Al-Hanbali, O.; Rutt, K. J.; Sarker, D. K.; Hunter, A. C.; Moghimi,
794 S. M. Concentration dependent structural ordering of poloxamine
795 908 on polystyrene nanoparticles and their modulatory role on
796 complement consumption. *J. Nanosci. Nanotechnol.* **2006**, *6*,
797 3126–3133.
- 798 (2) Ariola, F. S.; Krishnan, A.; Vogler, E. A. Interfacial rheology of
799 blood proteins adsorbed to the aqueous-buffer/air interface.
800 *Biomaterials* **2006**, *27*, 3404–3412.
- 801 (3) Avgoustakis, K.; Beletsi, A.; Panagi, Z.; Klepetsanis, P.; Livianous,
802 E.; Evangelatos, G.; Ithakissios, D.S. Effect of copolymer
803 composition on the physicochemical characteristics, in vivo stabil-
804 ity, and biodistribution of PLGA-mPEG nanoparticles. *Int.*
805 *J. Pharm.* **2003**, *259*, 115–127.
- 806 (4) Beaufilet, S.; Hadaoui-Hammoutène, R.; Vié, V.; Miranda, G.;
807 Perez, J.; Terriac, E.; Henry, G.; Delage, M.-M.; Léonil, J.; Martin,
808 P.; Renault, A. Comparative behavior of goat β and α_{s1} caseins
809 at the air-water interface and in solution. *Food Hydrocolloids*
810 **2007**, *21*, 1303–1330.
- 811 (5) Castelletto, V.; Cantat, I.; Sarker, D.; Bausch, R.; Bonn, D.;
812 Meunier, J. Stability of soap films: hysteresis and nucleation of
813 black films. *Phys. Rev. Lett.* **2003**, *90*, 483021–483024.
- 814 (6) Dauphas, S.; Beaumal, V.; Gunning, P.; Mackie, A.; Wilde, P.;
815 Vié, V.; Riaublanc, A.; Anton, M. Structures and rheological
816 properties of hen egg low density lipoprotein layers spread at the
817 air-water interface at pH 3 and 7. *Colloids Surf. B: Biointerfaces*
818 **2007**, *57*, 124–133.
- 819 (7) David, J. P.; Foegeding, E. A. Comparison of the foaming and
820 interfacial properties of whey protein isolate and egg proteins.
821 *Colloids Surf. B: Biointerfaces* **2007**, *54*, 200–210.
- 822 (8) Dimitrova, M. N.; Matsumura, H.; Dimitrova, A.; Neitchev, V. Z.
823 Interaction of albumins from different species with phospholipid
824 liposomes. Multiple binding sites. *Int. J. Biol. Macromol.* **2000**,
825 *27*, 187–194.
- 826 (9) Dos Santos, N.; Allen, C.; Doppen, A.-M.; Anantha, M.; Cox,
827 K. A. K.; Gallagher, R. C.; Karlsson, G.; Edwards, K.; Kenner,
828 G.; Samuels, L.; Webb, M. S.; Bally, M. B. Influence of
829 poly(ethylene glycol) grafting density and polymer length on
830 liposomes: relating plasma circulation to protein binding. *Biochim.*
831 *Biophys. Acta* **2007**, *1768*, 1367–1377.
- 832 (10) Erukova, V. Y.; Krylova, O. O.; Antonenko, Y. N.; Melik-
833 Nubarov, N. S. Effect of ethylene oxide and propylene oxide block
834 copolymers on the permeability of bilayer lipid membranes to
835 small molecules including doxorubicin. *Biochim. Biophys. Acta*
836 **2000**, *1468*, 73–86.
- 837 (11) Fleury, F.; Kudelina, I.; Nabiev, I. Interactions of lactone,
838 carboxylate and self-aggregated forms of camptothecin with
839 human and bovine serum albumins. *FEBS Lett.* **1997**, *406*, 151–
840 156.
- 841 (12) Frankel, E. N. Antioxidants in lipid foods and their impact on
842 food quality. *Food Chem.* **1996**, *57*, 51–55.
- 843 (13) Georgiev, G. A.; Sarker, D. K.; Al-Hanbali, O.; Georgiev, G. D.;
844 Lalchev, Z. Effects of poly(ethylene glycol) chains conformational
845 transition on the properties of mixed DMPC/DMPE-PEG thin
liquid films and monolayers. *Colloids Surf. B: Biointerfaces* **2007**,
59, 184–193.
- (14) Hill, K.; Horváth-Szancics, E.; Hajós, G.; Kiss, É. Surface and
interfacial properties of water soluble wheat proteins. *Colloids*
Surf. A: Physicochem. Eng. Aspects **2007**, . in press.
- (15) Krägel, J.; Wüstneck, R.; Müller, R.; Wilde, P. J.; Sarker, D. K.;
Clark, D. C. Assessment of surfactant monolayers at fluid
interfaces using a novel pendulum apparatus. *Colloids Surf.* **1995**,
113, Special Edition: Conference Proceedings of Bubble and Drop
95.
- (16) Mezdour, S.; Cuvelier, G.; Cash, M. J.; Michon, C. Surface
rheological properties of hydroxypropyl cellulose at air–water
interface. *Food Hydrocolloids* **2007**, *21*, 776–781.
- (17) Monroy, F.; Ortega, F.; Rubio, R. G.; Velande, M. G. Surface
rheology equilibrium and dynamic features at interfaces, with
emphasis on efficient tools for probing polymer dynamics at
interfaces. *Adv. Colloid Interface Sci.* **2007**, *134–135*, 175–189.
- (18) Péron, N.; Mészáros, R.; Varga, I.; Gilányi, T. Competitive
adsorption of sodium dodecyl sulphate and polyethylene oxide at
the air–water interface. *J. Colloid Interface Sci.* **2007**, *313*, 389–
397.
- (19) Pizza, L.; Gigli, J.; Bulbarelo, A. Interfacial rheology study of
espresso coffee foam structure and properties. *J. Food Eng.* **2008**,
84, 420–429.
- (20) Sarker, D. K. Sculpted nanoscale polymer films on micrometer
bubbles. *Curr. Nanosci.* **2005**, *1*, 157–168.
- (21) Sarker, D. K.; Wilde, P. J.; Clark, D. C. Competitive adsorption
of L- α -lysophosphatidylcholine/ β -lactoglobulin mixtures at the
interfaces of foams and foam lamellae. *Colloids Surf. B: Biointer-*
faces **1995**, *3*, 349–356.
- (22) Sarker, D. K.; Wilde, P. J.; Clark, D. C. Control of surfactant-
induced destabilization of foams through polyphenol-mediated
protein-protein interactions. *J. Agric. Food Chem.* **1995**, *43*, 295–
300.
- (23) Sarker, D. K.; Bertrand, D.; Chtioui, Y.; Popineau, Y. Charac-
terisation of foam properties using image analysis. *J. Texture Stud.*
1998, *29*, 15–42.
- (24) Sarker, D. K.; Axelos, M.; Popineau, Y. Methylcellulose-induced
stability changes in protein-based emulsions. *Colloids Surf. B:*
Biointerfaces **1999**, *12*, 147–160.
- (25) Sarker, D. K.; Wilde, P. J. Restoration of protein foam stability
through electrostatic propylene glycol alginate-mediated protein–protein
interactions. *Colloids Surf. B: Biointerfaces* **1999**, *15*, 203–213.
- (26) Vonarbourg, A.; Passirani, C.; Saulnier, P.; Benoit, J.-P. Param-
eters influencing the stealthiness of colloidal drug delivery
systems. *Biomaterials* **2006**, *27*, 4356–4373.
- (27) Wierenga, P. A.; Kosters, H.; Egmond, M. R.; Voragen, A. G. J.;
de Jongh, H. H. J. Importance of physical vs. chemical interactions
in surface rheology. *Adv. Colloid Interface Sci.* **2006**, *119*, 131–
139.
- (28) Wooster, T. J.; Augustin, M. A. Rheology of whey protein–dextran
conjugate films at the air/water interface. *Food Hydrocolloids*
2007, *21*, 1072–1080.

Received for review January 14, 2008. Revised manuscript received
March 11, 2008. Accepted March 12, 2008.

JF800122K